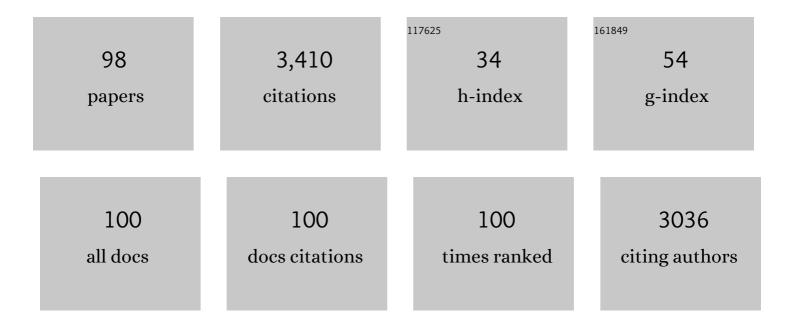
Guodong Jia

List of Publications by Year in descending order

Source: https://exaly.com/author-pdf/6395940/publications.pdf Version: 2024-02-01



CHODONC IM

#	Article	IF	CITATIONS
1	Archaeal tetraether lipids and their biphytane carbon isotope composition in sediments along an estuarine biogeochemical gradient. Geochimica Et Cosmochimica Acta, 2022, 318, 452-467.	3.9	2
2	In-situ provenance of brGDGTs in peat sediments: A case study from southern China and a comparison of global results. Organic Geochemistry, 2022, 167, 104373.	1.8	11
3	The distribution of intact polar lipid-derived branched tetraethers along a freshwater-seawater pH gradient in coastal East China Sea. Chemical Geology, 2022, 596, 120808.	3.3	6
4	Influence of water conditions on peat brGDGTs: A modern investigation and its paleoclimatic implications. Chemical Geology, 2022, 606, 120993.	3.3	6
5	Anthropogenic perturbations to the fate of terrestrial organic matter in a river-dominated marginal sea. Geochimica Et Cosmochimica Acta, 2022, 333, 242-262.	3.9	9
6	The nature, timescale, and efficiency of riverine export of terrestrial organic carbon in the (sub)tropics: Insights at the molecular level from the Pearl River and adjacent coastal sea. Earth and Planetary Science Letters, 2021, 565, 116934.	4.4	16
7	The Silurian-Devonian boundary in East Yunnan (South China) and the minimum constraint for the lungfish-tetrapod split. Science China Earth Sciences, 2021, 64, 1784-1797.	5.2	16
8	Lake-level records support a mid-Holocene maximum precipitation in northern China. Science China Earth Sciences, 2021, 64, 2161-2171.	5.2	14
9	Photosynthetic Production Determines Bottom Water Oxygen Variations in the Upwelling Coastal South China Sea Over Recent Decades. Frontiers in Earth Science, 2021, 9, .	1.8	1
10	Evaluation of environmental proxies based on long chain alkyl diols in the East China Sea. Organic Geochemistry, 2020, 139, 103948.	1.8	6
11	Cyclisation degree of tetramethylated brGDGTs in marine environments and its implication for source identification. Global and Planetary Change, 2020, 184, 103043.	3.5	14
12	Controlling factors and environmental significance of BIT and δ13C of sedimentary GDGTs from the Pearl River Estuary, China over recent decades. Estuarine, Coastal and Shelf Science, 2020, 233, 106534.	2.1	6
13	Long chain 1,14-diols as potential indicators for upper water stratification in the open South China Sea. Ecological Indicators, 2020, 110, 105900.	6.3	3
14	Consistent longâ€ŧerm Holocene warming trend at different elevations in the Altai Mountains in arid central Asia. Journal of Quaternary Science, 2020, 35, 1036-1045.	2.1	18
15	CO ₂ â€Induced Decoupling of Tropical Surface and Thermocline Water Temperature at the Onset of Interglacials. Geophysical Research Letters, 2020, 47, e2020GL088805.	4.0	2
16	Sedimentary core brGDGTs in the East China Sea are mainly produced in situ as evidenced by their similar distributions with brGDGTs derived from intact polar lipids. Organic Geochemistry, 2020, 149, 104095.	1.8	14
17	Operational Laboratory Methods for GDGTs Groups Separation. Journal of Ocean University of China, 2020, 19, 1073-1080.	1.2	0
18	lce formation on lake surfaces in winter causes warm-season bias of lacustrine brGDGT temperature estimates. Biogeosciences, 2020, 17, 2521-2536.	3.3	41

#	Article	IF	CITATIONS
19	Sedimentary records of nitrogen isotope in the western tropical Pacific linked to the eastern tropical Pacific denitrification during the last deglacial time. Geo-Marine Letters, 2020, 40, 89-99.	1.1	3
20	Late Eocene–Oligocene High Relief Paleotopography in the North Central Tibetan Plateau: Insights From Detrital Zircon U–Pb Geochronology and Leaf Wax Hydrogen Isotope Studies. Tectonics, 2020, 39, e2019TC005815.	2.8	32
21	Dispersal and aging of terrigenous organic matter in the Pearl River Estuary and the northern South China Sea Shelf. Geochimica Et Cosmochimica Acta, 2020, 282, 324-339.	3.9	27
22	Comparison of the U<sub>37</sub><sup>K<sup>â€ ² </sup&am LDI, TEX ₈₆ ^H , and RI-OH temperature proxies in sediments from the northern shelf of the South China Sea. Biogeosciences, 2020, 17, 4489-4508.	1p;gt;&ar 3.3	np;lt;/sup&am 20
23	Lipid biomarkers in suspended particulate matter and surface sediments in the Pearl River Estuary, a subtropical estuary in southern China. Science of the Total Environment, 2019, 646, 416-426.	8.0	42
24	Nitrogen Fixation Changes Regulated by Upper Water Structure in the South China Sea During the Last Two Glacial Cycles. Global Biogeochemical Cycles, 2019, 33, 1010-1025.	4.9	5
25	Spatiotemporal variation of organic geochemical properties since the mid-Miocene in the deep South China Sea (IODP Expedition 349). Journal of Asian Earth Sciences, 2019, 183, 103961.	2.3	3
26	Spatially different responses of nitrogen processing to precipitation during glacial-interglacial cycles on the Chinese Loess Plateau. Global and Planetary Change, 2019, 174, 164-171.	3.5	1
27	Assessment of sedimentary heterocyst glycolipids as tracers of freshwater input to the Changjiang Estuary and East China Sea. Chemical Geology, 2019, 521, 39-48.	3.3	6
28	Long chain diol index (LDI) as a potential measure to estimate annual mean sea surface temperature in the northern South China Sea. Estuarine, Coastal and Shelf Science, 2019, 221, 1-7.	2.1	7
29	Archaeal ammonia oxidation plays a part in late Quaternary nitrogen cycling in the South China Sea. Earth and Planetary Science Letters, 2019, 509, 38-46.	4.4	19
30	Seasonal variations of nitrate dual isotopes in wet deposition in a tropical city in China. Atmospheric Environment, 2019, 196, 1-9.	4.1	43
31	Sediment records of long chain alkyl diols in an upwelling area of the coastal northern South China Sea. Organic Geochemistry, 2018, 121, 1-9.	1.8	16
32	Intact polar glycosidic GDGTs in sediments settle from water column as evidenced from downcore sediment records. Chemical Geology, 2018, 501, 12-18.	3.3	10
33	The Sources and Transformations of Dissolved Organic Matter in the Pearl River Estuary, China, as Revealed by Stable Isotopes. Journal of Geophysical Research: Oceans, 2018, 123, 6893-6908.	2.6	25
34	High-relief topography of the Nima basin in central Tibetan Plateau during the mid-Cenozoic time. Chemical Geology, 2018, 493, 199-209.	3.3	22
35	Seasonal distribution of archaeal lipids in surface water and its constraint on their sources and the TEX ₈₆ temperature proxy in sediments of the South China Sea. Journal of Geophysical Research G: Biogeosciences, 2017, 122, 592-606.	3.0	27
36	A 15 ka pH record from an alpine lake in north China derived from the cyclization ratio index of aquatic brGDGTs and its paleoclimatic significance. Organic Geochemistry, 2017, 109, 31-46.	1.8	24

Guodong Jia

#	Article	IF	CITATIONS
37	Isoprenoid tetraether lipids in suspended particulate matter from the East China Sea and implication for sedimentary records. Organic Geochemistry, 2017, 114, 81-90.	1.8	15
38	Seasonal dynamics of particulate organic matter and its response to flooding in the <scp>P</scp> earl <scp>R</scp> iver <scp>E</scp> stuary, <scp>C</scp> hina, revealed by stable isotope (δ ¹³ <scp>C</scp> and δ ¹⁵ <scp>N</scp>) analyses. Journal of Geophysical Research: Oceans, 2017, 122, 6835-6856.	2.6	72
39	Differential timing of C 4 plant decline and grassland retreat during the penultimate deglaciation. Global and Planetary Change, 2017, 156, 26-33.	3.5	7
40	Asynchronous evolution of the isotopic composition and amount of precipitation in north China during the Holocene revealed by a record of compound-specific carbon and hydrogen isotopes of long-chain n-alkanes from an alpine lake. Earth and Planetary Science Letters, 2016, 446, 68-76.	4.4	65
41	A 15 ka lake water ÎƊ record from Genggahai Lake, northeastern Tibetan Plateau, and its paleoclimatic significance. Organic Geochemistry, 2016, 97, 5-16.	1.8	20
42	Investigating the long-term palaeoclimatic controls on the δD and δ180 of precipitation during the Holocene in the Indian and East Asian monsoonal regions. Earth-Science Reviews, 2016, 159, 292-305.	9.1	98
43	Catchment environmental change over the 20th Century recorded by sedimentary leaf wax n-alkane δ 13C off the Pearl River estuary. Science China Earth Sciences, 2016, 59, 975-980.	5.2	5
44	Reduced early Holocene moisture availability inferred from ÎƊ values of sedimentary <i>n</i> -alkanes in Zigetang Co, Central Tibetan Plateau. Holocene, 2016, 26, 556-566.	1.7	25
45	Warm season bias of branched GDGT temperature estimates causes underestimation of altitudinal lapse rate. Organic Geochemistry, 2016, 96, 11-17.	1.8	49
46	lsotopic evidence for the turnover of biological reactive nitrogen in the Pearl River Estuary, south China. Journal of Geophysical Research G: Biogeosciences, 2015, 120, 661-672.	3.0	53
47	Cooling trend over the past 4 centuries in northeastern Hong Kong waters as revealed by alkenone-derived SST records. Journal of Asian Earth Sciences, 2015, 114, 497-503.	2.3	16
48	Biogeochemical evidence of Holocene East Asian summer and winter monsoon variability from a tropical maar lake in southern China. Quaternary Science Reviews, 2015, 111, 51-61.	3.0	121
49	Reconstruction of a paleotemperature record from 0.3–3.7ka for subtropical South China using lacustrine branched CDGTs from Huguangyan Maar. Palaeogeography, Palaeoclimatology, Palaeoecology, 2015, 435, 167-176.	2.3	17
50	Paleoelevation of Tibetan Lunpola basin in the Oligocene–Miocene transition estimated from leaf wax lipid dual isotopes. Global and Planetary Change, 2015, 126, 14-22.	3.5	46
51	Different altitude effect of leaf wax n -alkane ÎƊ values in surface soils along two vapor transport pathways, southeastern Tibetan Plateau. Geochimica Et Cosmochimica Acta, 2015, 170, 94-107.	3.9	39
52	Seasonal variation in sources and processing of particulate organic carbon in the Pearl River estuary, South China. Estuarine, Coastal and Shelf Science, 2015, 167, 540-548.	2.1	73
53	Paleoenvironmental shifts and precipitation variations recorded in tropical maar lake sediments during the Holocene in Southern China. Holocene, 2014, 24, 1216-1225.	1.7	13
54	The development of late Holocene coastal cooling in the northern South China Sea. Quaternary International, 2014, 349, 300-307.	1.5	45

#	Article	IF	CITATIONS
55	Assessment of the difference between mid- and long chain compound specific Î'D-alkanes values in lacustrine sediments as a paleoclimatic indicator. Organic Geochemistry, 2014, 76, 104-117.	1.8	45
56	Carbon isotopic disequilibrium between seawater and air in the coastal Northern South China Sea over the past century. Estuarine, Coastal and Shelf Science, 2014, 149, 38-45.	2.1	1
57	Surface water δ180 in the marginal China seas and its hydrological implications. Estuarine, Coastal and Shelf Science, 2014, 147, 25-31.	2.1	12
58	Nitrate δ 15N and δ 18O evidence for active biological transformation in the Changjiang Estuary and the adjacent East China Sea. Acta Oceanologica Sinica, 2013, 32, 11-17.	1.0	14
59	Magnetic mineralogy and its implication of contemporary coastal sediments from South China. Environmental Earth Sciences, 2013, 68, 1609-1617.	2.7	12
60	Alkenone and tetraether lipids reflect different seasonal seawater temperatures in the coastal northern South China Sea. Organic Geochemistry, 2013, 58, 115-120.	1.8	38
61	Distribution of tetraether lipids in surface sediments of the northern South China Sea: Implications for TEX86 proxies. Geoscience Frontiers, 2013, 4, 223-229.	8.4	35
62	100-year ecosystem history elucidated from inner shelf sediments off the Pearl River estuary, China. Marine Chemistry, 2013, 151, 47-55.	2.3	35
63	An interlaboratory study of TEX ₈₆ and BIT analysis of sediments, extracts, and standard mixtures. Geochemistry, Geophysics, Geosystems, 2013, 14, 5263-5285.	2.5	76
64	Tetraether biomarker records from a loess-paleosol sequence in the western Chinese Loess Plateau. Frontiers in Microbiology, 2013, 4, 199.	3.5	65
65	Archaeal tetraether lipids record subsurface water temperature in the South China Sea. Organic Geochemistry, 2012, 50, 68-77.	1.8	78
66	Aeolian n-alkane isotopic evidence from North Pacific for a Late Miocene decline of C4 plant in the arid Asian interior. Earth and Planetary Science Letters, 2012, 321-322, 32-40.	4.4	21
67	A Holocene palaeomagnetic secular variation record from Huguangyan maar Lake, southern China. Geophysical Journal International, 2012, 190, 188-200.	2.4	20
68	Distributions and temperature dependence of branched glycerol dialkyl glycerol tetraethers in recent lacustrine sediments from China and Nepal. Journal of Geophysical Research, 2011, 116, .	3.3	72
69	Easterly denitrification signal and nitrogen fixation feedback documented in the western Pacific sediments. Geophysical Research Letters, 2011, 38, n/a-n/a.	4.0	18
70	Separation of total nitrogen from sediments into organic and inorganic forms for isotopic analysis. Organic Geochemistry, 2011, 42, 296-299.	1.8	16
71	Compound-specific hydrogen isotopes of long-chain n-alkanes extracted from topsoil under a grassland ecosystem in northern China. Science China Earth Sciences, 2011, 54, 1902-1911.	5.2	8
72	Is the maximum carbon number of long-chain n-alkanes an indicator of grassland or forest? Evidence from surface soils and modern plants. Science Bulletin, 2011, 56, 1714-1720.	1.7	34

#	Article	IF	CITATIONS
73	Terrestrial n-alkane signatures in the middle Okinawa Trough during the post-glacial transgression: control by sea level and paleovegetation confounded by offshore transport. Geo-Marine Letters, 2010, 30, 143-150.	1.1	9
74	Relationship between climatic conditions and the relative abundance of modern C3 and C4 plants in three regions around the North Pacific. Science Bulletin, 2010, 55, 1931-1936.	1.7	37
75	Monthly variations in nitrogen isotopes of ammonium and nitrate in wet deposition at Guangzhou, south China. Atmospheric Environment, 2010, 44, 2309-2315.	4.1	78
76	Assessment of soil <i>n</i> -alkane δ <i>D</i> and branched tetraether membrane lipid distributions as tools for paleoelevation reconstruction. Biogeosciences, 2009, 6, 2799-2807.	3.3	79
77	Nitrate sources and watershed denitrification inferred from nitrate dual isotopes in the Beijiang River, south China. Biogeochemistry, 2009, 94, 163-174.	3.5	149
78	CPI values of terrestrial higher plant-derived long-chain n-alkanes: a potential paleoclimatic proxy. Frontiers of Earth Science, 2009, 3, 266-272.	0.5	48
79	Spatial and seasonal variations in <i>δ</i> ¹³ C AND <i>δ</i> ¹⁵ N of particulate organic matter in a damâ€controlled subtropical river. River Research and Applications, 2009, 25, 1169-1176.	1.7	29
80	Compound specific Î'D values of long chain n-alkanes derived from terrestrial higher plants are indicative of the Î'D of meteoric waters: Evidence from surface soils in eastern China. Organic Geochemistry, 2009, 40, 922-930.	1.8	82
81	Variations in temperature and salinity of the surface water above the middle Okinawa Trough during the past 37kyr. Palaeogeography, Palaeoclimatology, Palaeoecology, 2009, 281, 154-164.	2.3	57
82	Soil <i>n</i> â€alkane <i>δ</i> ¹³ C along a mountain slope as an integrator of altitude effect on plant species <i>δ</i> ¹³ C. Geophysical Research Letters, 2009, 36, .	4.0	23
83	Evidence for the 8,200 a b.p. cooling event in the middle Okinawa Trough. Geo-Marine Letters, 2008, 28, 131-136.	1.1	20
84	Comparison of the carbon isotope composition of total organic carbon and long-chain n-alkanes from surface soils in eastern China and their significance. Science Bulletin, 2008, 53, 3921-3927.	9.0	31
85	Neutral monosaccharides as biomarker proxies for bog-forming plants for application to palaeovegetation reconstruction in ombrotrophic peat deposits. Organic Geochemistry, 2008, 39, 1790-1799.	1.8	56
86	Soil n-alkane ÎƊ vs. altitude gradients along Mount Gongga, China. Geochimica Et Cosmochimica Acta, 2008, 72, 5165-5174.	3.9	102
87	Sea surface temperature differences between the western equatorial Pacific and northern South China Sea since the Pliocene and their paleoclimatic implications. Geophysical Research Letters, 2008, 35, .	4.0	31
88	Sea surface temperature reconstruction for the middle Okinawa Trough during the last glacial–interglacial cycle using C37 unsaturated alkenones. Palaeogeography, Palaeoclimatology, Palaeoecology, 2007, 246, 440-453.	2.3	36
89	Contrast in surface water $\hat{l}'180$ distributions between the Last Glacial Maximum and the Holocene in the Southern South China Sea. Quaternary Science Reviews, 2006, 25, 1053-1064.	3.0	9
90	Distribution and sources of organic carbon, nitrogen and their isotopes in sediments of the subtropical Pearl River estuary and adjacent shelf, Southern China. Marine Chemistry, 2006, 98, 274-285.	2.3	234

#	Article	IF	CITATIONS
91	Reconstruction of surface ocean water pCO2(aq) in Nansha area, the South China Sea during the last 30 ka. Science Bulletin, 2003, 48, 199.	1.7	ο

Temporal and spatial variations in signatures of sedimented organic matter in Lingding Bay (Pearl) Tj ETQq0 0 0 rgBT $_{2.3}^{10}$ Overlock 10 Tf 50

93	Changes in terrestrial ecosystem since 30 Ma in East Asia: Stable isotope evidence from black carbon in the South China Sea. Geology, 2003, 31, 1093.	4.4	184
94	No aridity in Sunda Land during the Last Glaciation: Evidence from molecular-isotopic stratigraphy of long-chain n-alkanes. Palaeogeography, Palaeoclimatology, Palaeoecology, 2003, 201, 269-281.	2.3	40
95	Biological markers and their carbon isotopes as an approach to the paleoenvironmental reconstruction of Nansha area, South China Sea, during the last 30 ka. Organic Geochemistry, 2002, 33, 1197-1204.	1.8	35
96	Burial of Different Types of Organic Carbon in Core 17962 from South China Sea since the Last Glacial Period. Quaternary Research, 2002, 58, 93-100.	1.7	20
97	Sedimentary records of black carbon in the sea area of the Nansha Islands since the last glaciation. Science Bulletin, 2000, 45, 1594-1598.	1.7	8
98	Long-chain alkenones in Hotong Qagan Nur Lake sediments and its paleoclimatic implications. Science Bulletin, 1999, 44, 259-263.	1.7	23